HHS Public Access

Author manuscript

Sci Transl Med. Author manuscript; available in PMC 2018 December 06.

Published in final edited form as:

Sci Transl Med. 2018 June 06; 10(444): . doi:10.1126/scitranslmed.aap9736.

The antiprotease SPINK7 serves as an inhibitory checkpoint for esophageal epithelial inflammatory responses

Nurit P. Azouz[1], **Mario A. Ynga-Durand**[1,2], **Julie M. Caldwell**[1], **Ayushi Jain**[1], **Mark Rochman**[1], **Demetria M. Fischesser**[3], **Leanne M. Ray**[1], **Mary C. Bedard**[1], **Melissa K. Mingler**[1], **Carmy Forney**[4], **Matthew Eilerman**[1], **Jonathan T. Kuhl**[1], **Hua He**[5], **Jocelyn M. Biagini Myers**[6], **Vincent A. Mukkada**[7], **Philip E. Putnam**[7], **Gurjit K. Khurana Hershey**[6], **Leah C. Kottyan**[4], **Ting Wen**[1], **Lisa J. Martin**[5], and **Marc E. Rothenberg**[1,*]

[1]Division of Allergy and Immunology, Cincinnati Children's Hospital Medical Center, Department of Pediatrics, University of Cincinnati College of Medicine, Cincinnati, OH 45229-3026, USA

[2]Laboratorio de Inmunidad de Mucosas, Seccion de Investigacion y Posgrado, Escuela Superior de Medicina, Instituto Politecnico Nacional, Mexico City, Mexico

[3]Division of Molecular Cardiovascular Biology, Cincinnati Children's Hospital Medical Center, Department of Pediatrics, University of Cincinnati College of Medicine, Cincinnati, OH 45229-3026, USA

[4]Center for Autoimmune Genomics and Etiology, Cincinnati Children's Hospital Medical Center, Department of Pediatrics, University of Cincinnati College of Medicine, Cincinnati, OH 45229-3026, USA

[5]Division of Human Genetics, Cincinnati Children's Hospital Medical Center, Department of Pediatrics, University of Cincinnati College of Medicine, Cincinnati, OH 45229-3026, USA

[*]Corresponding author. rothenberg@cchmc.org.

Author contributions: N.P.A. designed and performed experiments, analyzed data, and wrote the paper. M.A.Y.-D. and J.M.C. assisted in experimental procedure and experimental design. A.J. and M.C.B. assisted in experimental procedure. M.R., H.H., L.C.K., and L.J.M. assisted in data analysis. D.M.F. performed experiments. L.M.R., J.T.K., J.M.B.M., V.A.M., P.E.P., and G.K.K.H. assisted in data collection. M.K.M. and M.E. assisted in data collection and experimental procedures. C.F assisted in experiments. T.W. assisted in data collection and experimental design. M.E.R. supervised the study.

Competing interests: T.W.'s institution has received an Aimmune research grant for other works, and they have an Eosinophilic Esophagitis Diagnostic Panel patent owned by Cincinnati Children's Hospital Medical Center (CCHMC). N.P.A., J.M.C., M.R., and M.E.R. are coinventors of patents owned by CCHMC. M.E.R. and N.P.A. are inventors on a pending U.S. provisional patent application (62/126,814) submitted by CCHMC that covers serine protease inhibitors for the treatment of EoE. M.E.R. and T.W. are inventors on granted U.S. patent 9,928,344 that covers diagnostic methods of EoE based on esophageal transcriptome analysis. M.E.R.'s institution has received a grant from the NIH for this work; they have grants for other works from a U.S.-Israel Binational Grant and Patient- Centered Outcomes Research Institute; they have patent ownership by CCHMC; he has received consultancy fees from Celgene, Genentech, Immune Pharmaceuticals, NKT Therapeutics, and PulmOne; he has received payment for lectures from Merck; and he has stock options with PulmOne, NKT Therapeutics, and Immune Pharmaceuticals. The rest of the authors declare that they have no competing interests.

Data and materials availability: RNA-seq expression data are publically available (GSE103356).

SUPPLEMENTARY MATERIALS

www.sciencetranslationalmedicine.org/cgi/content/full/10/444/eaap9736/DCl

Materials and Methods

References (40–46)

[6]Division of Asthma Research, Cincinnati Children's Hospital Medical Center, Department of Pediatrics, University of Cincinnati College of Medicine, Cincinnati, OH 45229-3026, USA

[7]Division of Gastroenterology, Hepatology and Nutrition, Cincinnati Children's Hospital Medical Center, Department of Pediatrics, University of Cincinnati College of Medicine, Cincinnati, OH 45229-3026, USA

Abstract

Loss of barrier integrity has an important role in eliciting type 2 immune responses, yet the molecular events that initiate and connect this with allergic inflammation remain unclear. We reveal an endogenous, homeostatic mechanism that controls barrier function and inflammatory responses in esophageal allergic inflammation. We show that a serine protease inhibitor, SPINK7 (serine peptidase inhibitor, kazal type 7), is part of the differentiation program of human esophageal epithelium and that SPINK7 depletion occurs in a human allergic, esophageal condition termed eosinophilic esophagitis. Experimental manipulation strategies reducing *SPINK7* in an esophageal epithelial progenitor cell line and primary esophageal epithelial cells were sufficient to induce barrier dysfunction and transcriptional changes characterized by loss of cellular differentiation and altered gene expression known to stimulate allergic responses (for example, *FLG* and *SPINK5*). Epithelial silencing of *SPINK7* promoted production of proinflammatory cytokines including thymic stromal lymphopoietin (TSLP). Loss of *SPINK7* increased the activity of urokinase plasminogen-type activator (uPA), which in turn had the capacity to promote uPA receptor-dependent eosinophil activation. Treatment of epithelial cells with the broad-spectrum antiserine protease, α1 antitrypsin, reversed the pathologic features associated with *SPINK7* silencing. The relevance of this pathway in vivo was supported by finding genetic epistasis between variants in *TSLP* and the uPA-encoding gene, *PLAU*. We propose that the endogenous balance between SPINK7 and its target proteases is a key checkpoint in regulating mucosal differentiation, barrier function, and inflammatory responses and that protein replacement with antiproteases may be therapeutic for select allergic diseases.

INTRODUCTION

Epithelial cells are uniquely positioned as the first line of defense against potential insults (*1*). In response to a perturbation of epithelial barrier integrity, acute injury, and/or immune stimulation, epithelial cells secrete an arsenal of proinflammatory, innate cytokines, such as interleukin-1 (IL-1), IL-25, IL-33, granulocyte-macrophage colony- stimulating factor, and thymic stromal lymphopoietin (TSLP), that can promote type 2 immune responses such as those that occur in allergic diseases (*1*).

The importance of the loss of barrier integrity in eliciting type 2 responses is illustrated by the atopic manifestations seen in individuals harboring loss-of-function mutations in the skin barrier proteins filaggrin (FLG) or desmoglein 1 (DSG1) (*2*). Although these geneticstudies provide proof of principle for the importance of barrier function in the elicitation of type 2 immunity, particularly in the skin, the relevance of these findings to the development of other allergic phenotypes besides atopic dermatitis remains uncertain. Furthermore, the mechanisms that link the associated barrier dysfunction with T helper cell 2 immunity

remain largely unknown. Here, we focused on uncovering the mechanism of allergic inflammation in eosinophilic esophagitis (EoE), a chronic, food-driven, inflammatory allergic disease of the esophagus (*3*). EoE is diagnosed according to the number of infiltrating eosinophils in the esophageal squamous epithelium, but other associated inflammatory cells are likely involved including mast cells, basophils, and lymphocytes (*4–6*). Besides being a recently emerging allergic disease that is in need of deeper understanding, EoE provides a unique opportunity to probe human allergic inflammation at the tissue level, as the diseased tissue is readily available for experimental investigation by routine endoscopic biopsies. Evidence is mounting that EoE is mediated by impaired barrier function, histologically observed as dilated intercellular epithelial spaces (*7*) and measurable by reduced epithelial resistance and increased paracellular permeability of esophageal biopsy samples (*8*). Multiple lines of emerging evidence substantiate a key role for the epithelium in the propagation and pathoetiology of EoE as the disease is mediated in part by loss of epithelial DSG1 (*9*). In addition, linkage of disease susceptibility with genetic variants in the epithelial genes *TSLP* (5q22) and *CAPN14* (2p23) has been established (*10*, *11*). Notably, IL-13 induces not only impaired barrier function in esophageal epithelium but also the gene product of *CAPN14*, calpain 14, an intracellular protease that is a key regulator of barrier function (*11*).

Proteins from the family of serine peptidase inhibitor, kazal type (SPINK) contain at least one inhibitory kazal domain that binds to their target serine proteases and inhibit their proteolytic function. *SPINK7* (also known as esophageal cancer-related gene 2) has a role as a tumor suppressor by its ability to inhibit the binding of urokinase plasminogen-type activator (uPA) to uPA receptor (uPAR) and cleavage of uPAR, which suppresses cell migration/invasion and signaling pathways including elevated cytosolic calcium (*12,13*).

Here, we demonstrate that the expression of SPINK7 is part of the epithelial cell differentiation program and that its deficiency induces epithelial cells to unleash proteolytic activity and proinflammatory innate responses associated with impaired epithelial barrier. Treatment with the broad-spectrum antiserine protease, α1 antitrypsin (A1AT), reversed the pathologic features associated with loss of *SPINK7.* Furthermore, we link these findings to the uPA/uPAR pathway by functional and genetic experiments. Together, we have identified a homeostatic anti-inflammatory mechanism in the esophagus and present evidence that its disruption may be a paramount signal in the development of disease and amenable to therapeutic targeting.

RESULTS

SPINK5 and *SPINK7* share low identity in their kazal domains and show differential expression in the esophagus

Of the eight *SPINK* genes expressed in the human esophagus, the most highly expressed were *SPINK5* and *SPINK7* [1450 and 831 fragments per kilobase million (FPKM), respectively; Fig. 1A]. Expression of *SPINK7* at homeostasis was >150-fold greater than that of *SPINK8* (831 versus 5 FPKM, respectively), which was the most highly expressed *SPINK* after *SPINK5* and *SPINK7.* Four of the eight expressed *SPINK*s were decreased in patients with EoE, with *SPINK7* showing the most significant down-regulation (16-fold

reduction; $P = 3 \times 10^{-8}$) and *SPINK5* showing 1.9-fold reduction (P = 0.0005) compared to control individuals (Fig. 1A). Having identified *SPINK5* and *SPINK7* as the most abundant *SPINKs* in the esophagus, we analyzed the identity between the inhibitory kazal domain of SPINK7 and the 15 kazal domains of SPINK5, known to be involved in the development of atopic dermatitis and type 2 immune responses (*14).* We found that the SPINK7 kazal domain shares the most identity with kazal domain 15 of SPINK5 (Fig. 1B) but with only 35% identity (fig. S1A). The average identity between the kazal domain of SPINK5 and the SPINK7 was lower compared to the identity between different kazal domains within SPINK5 (23 ± 5% compared to 42 ± 7%, respectively; fig. S1, A and B). Confocal microscopy of esophageal biopsies revealed that both SPINK5 and SPINK7 are expressed in the epithelium. SPINK5 and SPINK7 were expressed in all layers of the epithelium, with SPINK7 being more dominant in the suprabasal epithelium (Fig. 1C). Consistent with these data, we found some overlap but distinct spatial and cellular expression patterns of *SPINK5* and *SPINK7* in the esophageal tissue by single-cell RNA sequencing (RNA-seq). *SPINK5* was highly expressed in most epithelial cell types in the normal esophagus and colocalized with *KRT4,* whereas *SPINK7* was more abundant in a specific subset of cells that coexpressed *TGM3* (fig. S1C) identified by principal components analysis. In active EoE, *SPINK5* mRNA expression is moderately decreased but remains highly detectable in many cell types consistent with bulk RNA-seq data, whereas SPINK7 is nearly completely undetectable. These data further support the different roles of SPINK5 and SPINK7 in the esophagus.

Consistent with previous reports, SPINK5 protein expression was down-regulated in EoE patients compared to control individuals (*15, 16*), but this effect was modest compared with SPINK7, which was almost completely lost in patients with EoE compared to control individuals (Fig. 1C). Analysis of additional esophageal biopsies (n = 133 patients) demonstrated that *SPINK7* mRNA was down-regulated in EoE compared to controls (Fig. 1D) (*17*). Because it had been demonstrated that EoE pathogenesis is mediated at least in part by an IL-13- stimulated, keratinocyte-derived transcriptome (*18*), we also asked whether IL-13 can down-regulate *SPINK5* and *SPINK7*expression. IL-13 stimulation up-regulated *CCL26* as expected in differentiated esophageal epithelial progenitor cells (EPC2), but IL-13 did not alter *SPINK5* and *SPINK7* expression (Fig. 1E).

Notably, SPINK7 expression is reinstated with successful therapy (that is, patients with inactive disease after treatment with diet or glucocorticosteroids) as compared to patients who were diagnosed with active disease after treatment (Fig. 1F). *SPINK7* correlated with 73 EoE signature genes. *SPINK7* positively correlated with key barrier genes such as *CRISP3, CLDN10, DSG1,* and *FLG* and negatively correlated with the genes of key esophageal related cytokines/chemokines and inflammation such as *CCL26, CXCL1, CXCL6, CXCL8,* and *ALOX15;* genes that have functions involved in tissue remodeling such as *MMP12, CTSC, PLAU, PLAUR,* and *POSTN;* mast cell proteases including *CPA3* and *TPSB2;* and the ion channels *ANO1* and *SLC16A4* (Fig. 1G and table S1). In contrast to *SPINK7, SPINK5* correlated with a smaller number of genes (17 genes). These genes include *CLDN10, CRISP2, CRISP3, UPK1A, CRYM,* and *ARG1* (Fig. 1G and table S1). *SPINK7* and *SPINK5* correlated with each other and with other EoE signature genes including *CCL26, CDH26, IL5, CLDN10, MMP12,* and *CXCL8* (Fig. 1G and table S1).

SPINK5 and *SPINK7* expression is part of the epithelial differentiation program and regulates barrier function, whereas loss of *SPINK7* is upstream of *SPINK5* and impairs epithelial differentiation

We induced epithelial differentiation by culture of esophageal epithelial progenitor cell line (EPC2) exposed to the air-liquid interface (ALI), as previously reported (*9*). Among *SPINK* family members, the expression of *SPINK5* and *SPINK7* mRNA was most highly increased with differentiation, increasing by 915- and 752-fold, respectively (P = 0.0007 and $P < 10^{-10}$, respectively; fig. S2A), consistent with the in vivo expression pattern.

We aimed to silence *SPINK5* and *SPINK7* expression specifically by interference short hairpin RNA (shRNA) targeting of a region of *SPINK5* and *SPINK7* that exhibited less conservation between both genes (fig. S2B). EPC2 cells and primary esophageal epithelial cells from control subjects were stably transduced with a vector expressing either shRNA targeting *SPINK5* or *SPINK7* or nonsilencing control (NSC) shRNA. In cells expressing the *SPINK7*-directed shRNA, a nearly complete loss of *SPINK7* expression and no effect on *SPINK5* were observed, and silencing of *SPINK5* did not alter *SPINK7* expression, indicating specificity of the gene-silencing constructs toward *SPINK5* and *SPINK7* (fig. S2C). The silencing of either *SPINK5 or SPINK7* resulted in dilated intercellular spaces after ALI differentiation (day 14) compared with NSC treatment (Fig. 2A). Transepithelial electrical resistance (TEER) was reduced by ~2.3- and ~2.5-fold (both $P < 0.0001$) during ALI differentiation of *SPINK7*- and *SPINK5*-silenced cells compared to NSC-treated cells, respectively (Fig. 2B). These data collectively suggest that silencing of either *SPINK7* or *SPINK5* is sufficient to impair the epithelial barrier.

Having identified both *SPINK7* and *SPINK5* as part of the epithelial differentiation program (fig. S2A), we aimed to examine the effect of *SPINK7* silencing on *SPINK5* expression and vice versa. There was no effect of *SPINK7* down-regulation on *SPINK5* mRNA abundance in undifferentiated EPC2 cells (fig. S2C), whereas *SPINK7* silencing markedly reduced the expression of *SPINK5* mRNA after ALI differentiation (88-fold decrease; Fig. 2C). In contrast, *SPINK5* silencing did not affect *SPINK7* expression after ALI differentiation (Fig. 2D). Notably, the expression of *SPINK7* correlated with *SPINK5* in a cohort of EoE patients (n = 84, $r = 0.75$, $P < 0.0001$; fig. S2D). These data suggest that loss of *SPINK7* expression may be upstream of loss of *SPINK5.*

We performed whole-transcriptome sequencing analysis of EPC2 cells after ALI differentiation. This analysis revealed 270 genes that were differentially expressed (DE) in the *SPINK7*-silenced cells compared to NSC-treated cells [$P < 0.05$, fold change > 2, reads per kilobase of transcript, per million mapped reads (RPKM) > 1; table S2]. The modified genes were enriched for those involved in epidermal differentiation, inflammation, and skin physiology, including the transcription factors *STAT1* and *NFATC2* and cytokines such as *IL23, IL37,* and *CCL24,* and included decreased expression of *FLG, FLG2, LOR,* keratins, transglutaminases, and IL-36 receptor antagonist *(IL36RN)* (fig. S3A and table S2). Collectively, these findings provide evidence that loss of *SPINK7* regulates type 1 interferon responses (fig. S3B). Furthermore, we compared gene expression between EPC2 monolayer culture (day 0 of differentiation) and differentiated EPC2 cells in ALI culture (day 14 of differentiation). This analysis revealed 3225 DE genes ($P < 0.05$, fold change > 2, RPKM >

1; table S3). The majority (77%) of the genes modified by *SPINK7* silencing were also modulated during epithelial cell differentiation, including a regulator of terminal epidermal differentiation, calmodulin-like 5 *(CALML5)* (*19*), and the cornified envelope components expressed by differentiated keratinocytes, such as *FLG* and *LOR* (fig. S3C shows the top dysregulated genes that overlap between differentiation and *SPINK7* silencing). The genes that were increased the most during differentiation were down-regulated after *SPINK7* silencing, indicating that loss of *SPINK7* promotes transcriptional changes that mimic an undifferentiated epithelial phenotype.

Focusing on the epidermal differentiation complex (EDC) on 1q21, the locus with the greatest changed expression in the EoE transcriptome (*20*), we intersected the genes altered by *SPINK7* silencing and the EDC. Of the 54 EDC genes expressed by differentiated epithelial cells (RPKM > 1), 17 genes were significantly down-regulated ($P < 0.05$) by *SPINK7* silencing (Fig. 2E). *SPINK7* silencing resulted in a marked decrease in *FLG* mRNA and protein expression (Fig. 2, F to H).

We analyzed the architectural changes after *SPINK7* loss. At baseline (day 7), *SPINK7* silencing increased noncellular spaces by 5.4-fold ($P = 0.008$) compared to NSC treatment, which yielded densely packed cells (fig. S4A). The same finding was observed in SPINK7-silenced cells at day 9 (5.4-fold increase; $P = 0.01$). Notably, by 11 to 14 days, blebbing of the squamous layers was seen after *SPINK7* silencing (fig. S4A). Quantifying the percentage of total area of dilated intercellular spaces revealed that *SPINK7*-silenced cells had a threefold increase ($P = 0.0001$) in the noncellular tissue area compared with that of NSC-treated cells (fig. S4A). As a control, morphometric analysis of the total area of the differentiated cells was not altered after *SPINK7* silencing compared to NSC treatment (fig. S4B), indicating no change in acanthosis. Transmission electron microscopy revealed that the microplicae, intercellular ridges, and finger-like projections between cells that were readily apparent in the NSC-treated cells were nearly absent from *SPINK7*-silenced cells (Fig. 2I).

Immunofluorescence analysis of submerged and ALI cultures of EPC2 cells revealed that E-cadherin localized to the cellular membrane and showed an organized pattern of cellular junctions in NSC- treated cells (Fig. 2J). After *SPINK7* silencing, E-cadherin was diffusely present within cells and the cellular membrane, and the staining was often found in aggregates (Fig. 2J). Immunofluorescence analysis of DSG1 expression in ALI cultures of NSC-treated cells revealed mainly membrane localization, whereas DSG1 expression was decreased and localized in the cytoplasm and membrane after *SPINK7* silencing (Fig. 2K). This is relevant because DSG1 is markedly lost in EoE (*9*), and homozygous mutations in *DSG1* are sufficient for induction of EoE (*2*).

Confocal microscopic analysis of high-resolution three-dimensional structures of differentiated cells revealed that DSG1 and E-cadherin staining was limited to membranes in the superficial regions of the NSC-treated cells and demonstrated close association between the cells (Fig. 2L and movie S1). In contrast, there was separation of these molecules after *SPINK7* silencing (Fig. 2L and movie S2), with a 3.5-fold increase in the ratio of cells with altered junctional proteins after *SPINK7* silencing compared to NSC treatment ($P = 1.6 \times$

10^{-10}; fig. S4C). These collective data demonstrate that loss of *SPINK7* results in epithelial acantholysis.

Analysis of the transcellular permeability, as measured by the flux of macromolecules [fluorescein isothiocyanate (FITC)-dextran], was significantly increased in *SPINK7*-silenced cells compared to NSC shRNA-treated cells, exhibiting a 2.9-fold increase at 3 hours ($P = 6.8 \times 10^{-5}$; fig. S4D). These data reveal that *SPINK7* silencing expression was sufficient to induce impaired barrier function.

Silencing of *SPINK7* results in transcriptional changes that overlap with the EoE and IL-13-associated transcriptomes

We examined the impact of loss of *SPINK7* on the EoE transcriptome, which is the altered transcriptional profile of esophageal tissue of patients with EoE compared to healthy controls (*18*). We intersected the genes modified by *SPINK7* silencing in differentiated cells with the EoE transcriptome and found a substantial overlap of 36% (Fig. 3A). These genes were enriched for functional pathways involved in skin inflammation, skin physiology, skin morphology, and innate immune response (Fig. 3A), including major histocompatibility complex (MHC), *FLG,* interferon induced with helicase C domain 1 *(IFIH1),* and *IL36RN* genes (fig. S5A). Because it had been demonstrated that EoE pathogenesis is mediated at least in part by an IL-13-stimulated, keratinocyte-derived transcriptome (*18*), we also intersected the genes modified by *SPINK7* silencing with the genes modified by IL-13 treatment in EPC2 cells after ALI differentiation using genome-wide RNA-seq (21). This is a relevant transcriptome set as humanized anti-IL-13 therapy has a beneficial impact on patients with EoE (22). One hundred nineteen genes (44% of the genes in the SPINK7 transcriptome) overlapped between these two transcript profiles (Fig. 3B). These genes were enriched for skin pathways including keratosis and acantholysis, skin development and differentiation, and innate immunity pathways (Fig. 3B and fig. S5B). Many of the genes were localized in the cornified envelope (Fig. 3B). Further, nearly half of the overlapping genes between *SPINK7*-regulated transcripts and the EoE transcriptome were regulated by IL-13 (Fig. 3C).

SPINK7 silencing unleashes the production of proinflammatory cytokines

We analyzed the supernatant of SPINK7-silenced cells using a multiplex cytokine array. Among 64 cytokines, there was a marked change in 18 cytokines (Fig. 4A and fig. S6A). IL-8, a potent chemoattractant of neutrophils and eosinophils (*23*), was increased by 12-fold ($P = 0.03$) in the *SPINK7-silenced* cells compared to NSC-treated cells (Fig. 4A). The increase in IL-8 was verified by enzyme-linked immunosorbent assay and quantitative PCR analysis (Fig. 4B and fig. S6B). There was a negative correlation between *SPINK7* and *IL8* mRNA expression in the esophageal biopsies of a cohort of patients with and without active EoE ($n = 83$ and $n = 50$, respectively, $P = 0.014$; fig. S6C), supporting the inverse relationship between *SPINK7* and *IL8.* In addition, *IL8* expression increased in patients with EoE compared to controls (fig. S6D), consistent with a previous report (*24).* Last, loss of *SPINK7* also stimulated TSLP release via Toll-like receptor 3 (TLR3) activation (Fig. 4C).

CRISPR/Cas9-generated CRISPR/Cas9 *SPINK7* knockout cells exhibit similar phenotypes to SPINK7-silenced cells, overexpress the mesenchymal marker vimentin, and exhibit increased metalloprotease activity

To validate the role of SPINK7 in epithelial homeostasis, we generated SPINK7-deficient EPC2 cells via clustered regularly interspaced short palindromic repeats (CRISPR)/Cas9-mediated genome editing. CRISPR/Cas9 induced insertions and deletions in both alleles, resulting in a frameshift and premature stop codon after amino acid 17 (fig. S7, A and B). In contrast to shRNA SPINK7-silenced cells that expressed low *SPINK7,* CRISPR/Cas9 *SPINK7* knockout (KO) cells did not express detectable SPINK7 protein after differentiation compared to control cells as assessed by Western blot analysis (fig. S7C). After differentiation, *SPINK7* KO cells demonstrated a twofold decrease in the TEER compared to control cells ($P < 0.0001$; Fig. 5A). The impaired barrier was associated with decreased *FLG* mRNA expression (Fig. 5B). Supernatants of differentiated control cells inhibited the activity of purified uPA (70% inhibition; Fig. 5C). In contrast, supernatants of *SPINK7* KO cells had increased uPA activity (Fig. 5C). *SPINK7* KO cells had increased TSLP release compared to control cells after TLR3 stimulation (Fig. 5D). We observed a marked increase in vimentin expression in the *SPINK7* KO cells (Fig. 5, E and F), a marker of mesenchymal cells. In addition, we observed increased production of transforming growth factor-β by SPINK7 KO epithelial cells (fig. S7D), which may explain the increased vimentin expression (*25).* Therefore, we suggest that loss of SPINK7 promotes epithelial-to-mesenchymal transition (EMT), at least in part.

SPINK7 was identified as an esophageal tumor suppressor gene because of its protein's ability to inhibit invasion of tumor cells by inhibiting the degradation of the extracellular matrix (ECM) (*13).* We further investigated whether SPINK7 could indirectly affect ECM processes by regulating the activity of matrix metalloproteinases (MMPs), which are important regulators of the ECM rearrangement. CRISPR/Cas9 *SPINK7* KO supernatants demonstrated significantly higher MMP proteolytic activity as assessed by the cleavage of MMP fluorogenic substrate (23% increased; $P = 0.008$; Fig. 5G). We then used a fluorogenic substrate for MMP9 and observed significantly increased MMP9 activity (twofold increased; $P = 0.0048$; Fig. 5H).

We performed a whole-transcriptome sequencing analysis of CRISPR/Cas9 gene-edited *SPINK7* KO cells compared to control cells after ALI differentiation. We identified 1498 genes that were dysregulated in the *SPINK7* KO cells compared to control cells (table S4). These genes were enriched with genes that regulate skin development, defense response, response to cytokines and inflammatory response, keratinocytes differentiation, cell death, wounding, and cell migration (Fig. 5I). In addition, these genes overlapped with 51% of the *SPINK7*-silenced cells transcriptome (139 genes; fig. S7E). Notably, *SPINK7* KO cells overexpressed the gene product of the EoE susceptibility locus, *CAPN14* (table S4) (26).

SPINK7/uPA/uPAR pathway contributes to eosinophil activation

Supernatants from cells during differentiation revealed a 1.8-fold increase in uPA activity after *SPINK7* silencing ($P = 0.013$; Fig. 6A), consistent with the reported inhibitory activity of SPINK7 (12, 13). In esophageal biopsies from patients with EoE, uPA mRNA expression

was increased by 2.7-fold (P = 0.0003) and uPA activity was increased by 10-fold (P = 0.043) compared to control individuals (Fig. 6, B and C). As a control, pan protease activity was not altered in EoE biopsies compared to control biopsies (Fig. 6D), indicating a relatively specific effect on uPA.

We investigated the effect of uPA on EPC2 during ALI. The uPA activity in the cell supernatant was substantially elevated by uPA administration in a dose-dependent manner (fig. S8A). uPA did not affect the barrier function as measured by TEER (fig. S8B) and did not induce dilated intercellular spaces (fig. S8C). uPA did not modify the expression of a panel of EMT markers in EPC2 cells (fig. S8D).

uPA activates eosinophils

We analyzed the expression of uPAR, the uPAR on immune cells that are involved in EoE including mast cells, eosinophils, basophils, and CD4 and CD8 lymphocytes from the blood and esophagus (fig. S9A). The highest expression of uPAR was found on blood eosinophils (fig. S9, affect the levels of cell surface D2D3 domain (fig. S9, C and D). We then showed that supernatants derived from CRISPR/Cas9 *SPINK7* KO cells after differentiation had the capacity to decrease the D1 domain on the surface of eosinophils compared to supernatants derived from differentiated control cells (Fig. 6E). Furthermore, we detected down-regulation of uPAR on esophageal eosinophils in the biopsies of patients with EoE compared with blood eosinophils ($P = 5 \times 10^{-5}$; Fig. 6F and fig. S9B). We further analyzed the expression of the D2D3 domain on eosinophils using an antibody that binds to the D3 domain. In contrast to the D1 domain, the expression of the D2D3 domain was detectable in esophageal eosinophils (Fig. 6G). These collective data indicate that uPAR is expressed by esophageal eosinophils and is modulated in its D1 domain in the esophagus and that loss of SPINK7 initiates downstream events that have the capacity to modulate the D1 domain. Notably, uPA stimulated activation of eosinophils as measured by release of eosinophil peroxidase (EPX) (P = 0.0007) from peripheral blood-derived eosinophils (Fig. 6H). In addition, supernatants from CRISPR/Cas9 gene-edited *SPINK7* KO cells stimulated activation of eosinophils that was higher by 26-fold compared to supernatants from control cells (P = 0.002; Fig. 6H). These results indicate that in EoE, esophageal eosinophils express uPAR that is likely being cleaved by uPA in the esophagus and that this process has potential to promote eosinophil activation (fig. S9E).

Administering a protease inhibitor reverses the effects caused by loss of *SPINK7*

We hypothesized that inhibiting elevated proteolytic activity would ameliorate the impaired barrier and the loss of epithelial differentiation elicited by the loss of *SPINK7.* We focused our attention on a pharmacological drug with a broad serine protease inhibition activity using the A1AT (27). Administering A1AT to differentiated EPC2 cells inhibited the trypsin-like activity of the supernatant of *SPINK7*-silenced cells (Fig. 7A). A1AT dose-dependently improved barrier function (Fig. 7B) and epithelial integrity as demonstrated by the decreased dilation of intercellular spaces (Fig. 7C). Consistent with these findings, treatment with A1AT increased FLG expression (Fig. 7D).

Single-nucleotide polymorphism screen reveals genetic epistasis between *TSLP* and *PLAU*

Epistasis occurs when the effect of a genetic variant on a trait is dependent on genotypes of other variants elsewhere in the genome (*28).* We screened for epistasis between *TSLP,* located at 5q22, an established EoE-associated genetic locus (10, *29)* and atopy-associated genes (n = 68) using a custom, high-density, single-nucleotide polymorphism (SNP) chip platform, allowing us to potentially identify genetic interactions. Using logistic regression with an interaction term, we screened for evidence of epistasis between *TSLP* and atopy-associated genes on the SNP chip using EoE (n = 725) and control (n = 412) cohorts. We found an unexpected, strong association between *PLAU* (uPA) variants and a major EoE genetic susceptibility variant at 5q22 locus within the *TSLP* locus. The most substantial SNPs that interacted with *TSLP* were three *PLAU* variants (rs2459449, rs2227551, and rs2227564; *P* value range, 0.0001 to 0.0003; Fig. 8A).

To evaluate the interaction further, we created a four-level variable that characterized the presence of at least one minor allele for *TSLP* and *PLAU* (rs2459449). We then performed logistic regression and found that the absence of the *TSLP* minor allele [*TSLP* risk variant (C/C)] in combination with the presence of the minor allele [(C/T) or (T/T)] in *PLAU* increased the risk of EoE [odds ratio (OR) = 2.73; *P* = 0.0003] compared to individuals who had both minor alleles (Fig. 8B). The absence of the minor allele from *PLAU* resulted in a modest increase in EoE risk (OR = 1.56), as did the absence of minor alleles from both genes (OR = 1.29). These collective data support an interaction between TSLP and the *SPINK7/PLAU* pathway.

DISCUSSION

The data presented here identify a role for the naturally occurring serine protease inhibitor SPINK7 as a homeostatic, anti-inflammatory regulator of esophageal epithelium. We demonstrate that SPINK5 and SPINK7 are constitutively produced by differentiated esophageal squamous epithelium. Loss of *SPINK7* is sufficient for induction of proinflammatory responses including (i) loss of barrier integrity including formation of dilated intercellular spaces, absence of microplicae, increased paracellular permeability, and reduced TEER; (ii) epithelial acantholysis including disruption of the adherens junction proteins E-cadherin and DSG1; (iii) defective epithelial cell differentiation highlighted by loss of *FLG* expression; (iv) promotion of the EMT marker vimentin and metalloproteinases; and (v) induction of an innate transcript signature that overlaps with allergic inflammation including processes regulated by IL-13 and marked cytokine release. We identify uPA as a mediator of eosinophil activation downstream from the loss of *SPINK7,* at least in vitro. Finally, we substantiate these findings by identifying genetic epistasis between *PLAU* and *TSLP.*

SPINK5 undoubtedly contributes to type 2 immune responses, as demonstrated by the hyperatopy state when *SPINK5* deficiency occurs in the rare autosomal recessive disease Netherton syndrome (*14, 30).* Recently, a high prevalence of esophageal eosinophilia was observed in a cohort of patients with Netherton syndrome (15, *16).* We showed that *SPINK5* and *SPINK7* are expressed in the epithelium but exhibit distinct spatial and cellular expression patterns. In active EoE, *SPINK5* expression is decreased but still detectable,

whereas *SPINK7* expression is virtually abolished at the single-cell level. We have shown that although SPINK5 and SPINK7 share low percent identity in the protein sequences, silencing of either *SPINK7* or *SPINK5* is sufficient to impair the epithelial barrier in a similar matter. Although SPINK5's role in skin atopic diseases has been highly investigated, the role of SPINK7 in atopic diseases is less clear. The comparative importance of SPINK7 in the context of EoE is demonstrated by its relative deficiency in EoE compared with control individuals and its high expression in the normal esophagus. Analysis of esophageal-specific genes in public data sets reveals that *SPINK7* is an esophageal enriched gene (31).

We demonstrated that uPA activity increases in EoE biopsies, suggesting that decreased SPINK7 inhibitory activity is present in EoE. However, uPA is inhibited by other protease inhibitors beside SPINK7,and therefore, loss of *SPINK7* may only partially account for the increased uPA activity. Whether SPINK5 kazal domains can inhibit uPA requires further investigations. We could not directly determine the activity of SPINK5 and SPINK7 in the esophagus due to overlap and unknown identity of target proteases. Our data reveal decreased expression of *SPINK7,* and we suggest that this decreased expression accounts for dysregulation in proteolysis in the esophagus. We further provide evidence that loss of *SPINK7* in differentiated EPC2 cells may be upstream from loss of *SPINK5.* However, we cannot exclude the possibility that complete loss of *SPINK5* expression alters epithelial differentiation and subsequently affects SPINK7 expression. Lack of FLG and DSG1 are also contributory to barrier impairment (fig. S10A) (9, *32*), but their silencing was not sufficient for loss of *SPINK7* (fig. S10B).

We further demonstrate that esophageal eosinophils lack the D1 domain of uPAR that is normally observed on blood eosinophils. In addition, our data demonstrate that uPA directly activates eosinophils, perhaps by cleaving uPAR. These findings indicate that SPINK7 has a potential to regulate the interplay between epithelial cells and eosinophils in the esophagus. Further, genetic epistasis between *TSLP* and *PLAU* alleles provides independent evidence for the contribution of this pathway to allergic inflammation in EoE.

It has been reported that SPINK7 provides a spindle assembly checkpoint and that loss of *SPINK7* results in rapid proliferation and chromosomal instability (33). Therefore, we suggest that the defect in the differentiation process caused by the loss of *SPINK7* could be a part of a programmed cell response to repair damaged tissue by increasing the pool of undifferentiated cells with proliferative capacity. In addition, we demonstrate that the loss of *SPINK7* caused release of several cytokines [that is, IL-1β, TNFα (tumor necrosis factor-α), and PDGF (platelet-derived growth factor)] that are key regulatory molecules of tissue repair. The uPA/uPAR pathway has been shown to potentially interact with these cytokines in wound repair mechanisms (*34, 35).* Furthermore, IL-8 is known to regulate tissue regeneration by promoting angiogenesis (34, 36). Notably, induced angiogenesis and IL-8 occur in EoE (24, 37).

Although SPINK7 loss induces a transcript signature that overlaps with processes regulated by IL-13, IL-13 stimulation does not affect *SPINK7* expression. We suggest that SPINK7 regulates a unique pathway that occurs in parallel to IL-13-induced changes. The question as to what causes the down-regulation of *SPINK7* in EoE remains unanswered.

It has been reported that SPINK7 regulates its function by controlling the RNA binding protein human antigen R (HuR) (38). HuR increases the expression of its target proteins by binding to AU-rich sequences in 3′ untranslated regions on the mRNAs and preventing mRNA degradation. HuR regulates the expression of eotaxin-1, which is a potent chemoattractant of eosinophils (39). The involvement of the SPINK7/HuR pathway in EoE requires further investigation.

We suggest that loss of *SPINK7* serves a causative role in compromising the epithelial barrier and as an internal signal for epithelial damage with inflammatory consequences. We propose that SPINK7 provides a novel checkpoint for dampening a proinflammatory response characterized by excessive cytokine production and eosinophil activation in the esophagus. In addition, genetic variants in this pathway interact with pathways germane to allergic responses (that is, *TSLP*) to initiate and/or propagate allergic inflammation at least in the esophagus. We demonstrate that administering the serine protease inhibitor A1AT ameliorates the epithelial impairment in vitro, at least in part. Thus, we propose that protein replacement therapy with protease inhibitors such as A1AT has therapeutic potential for atopic diseases such as EoE and Netherton syndrome. A limitation of our study is that our findings are primarily done in vitro; further testing in preclinical in vivo models and, eventually, in patients is necessary before conclusions are definitive.

We suggest that local fluctuations in *SPINK7* expression regulate allergic responses by three mechanisms: first, by hampering the epithelial barrier, which promotes immune cells (such as dendritic cells) to increasingly encounter luminal antigens; second, by regulating uPA activity and modulating uPAR on the surface of eosinophils; and third, by priming epithelial cells to secrete proallergic and immunomodulatory cytokines (illustrated in fig. S10C). Given these collective observations, we propose that SPINK7 is a counterregulatory antiprotease that curtails inflammatory responses in the squamous epithelium, particularly in the esophagus. Acquired loss of *SPINK7* is sufficient for unleashing a series of responses that induce marked proinflammatory innate immunity, contributing to the allergic response in this tissue. A deeper understanding of the reported findings and their in vivo relevance is warranted.

MATERIALS AND METHODS

Study design

The aims of this study were to assess whether the loss of esophageal *SPINK7* has a role in the initiation and/or propagation of EoE and to understand the mechanism by which SPINK7 mediates its function. We analyzed *SPINK7* mRNA and protein expression in the esophagus using several cohorts of EoE patients compared to controls in comparison to other SPINK members, particularly *SPINK5.* We complement these analyses with sequence homology analysis between SPINK7 kazal domains and SPINK5 kazal domains. We manipulated *SPINK7* expression in EPC2 cells and in primary cells derived from esophageal biopsies using shRNAs and by CRISPR/ Cas9 gene deletion. Epithelial cells were differentiated and assessed by several experimental approaches including FITC-dextran flux, epithelial resistance measurements, immunofluorescence (IF) analysis of barrier proteins and junctional complexes, proteolytic activity, electron microscopy examination, and cytokine

release. Whole- transcriptome analysis was carried out in differentiated EPC2 cells after *SPINK7* silencing compared to NSC and in CRISPR/Cas9 *SPINK7* KO compared to control.

uPA proteolytic activity was determined in biopsies of EoE patients and control patients, and uPAR expression was assessed in several immune cells. We investigated the effect of loss of *SPINK7* and increased uPA activity on eosinophils by analyzing uPAR cleavage by flow cytometry and eosinophil degranulation by EPX release. Eosinophils were incubated with recombinant uPA or with supernatants derived from differentiated CRISPR/Cas9 *SPINK7* KO or controls. Lastly, we used a custom Illumina GoldenGate SNP chip that contains 668 SNPs in 78 genes and performed logistic regression analyses with interaction term using 725 cases and 412 controls. Information on the study outline, sample size, and statistical analysis is shown in the main text, figures, figure legends, and the Supplementary Materials.

Statistical analysis

Statistical significance was determined using a *t* test (unpaired, twotailed) unless mentioned otherwise. Spearman correlations were used to test for correlated gene expression. All statistical analyses were performed using GraphPad Prism (GraphPad Software Inc.).

Supplementary Material

Refer to Web version on PubMed Central for supplementary material.

Acknowledgments:

We thank A. Rustgi (University of Pennsylvania) for the human telomerase reverse transcriptase-immortalized EPC2 cell line, M. Kofron (Cincinnati Children's Hospital) for assistance in confocal image analysis, M. Weirauch (Cincinnati Children's Hospital) for advising on SNP analysis, A. Munitz (Tel Aviv University) for insightful discussion, and M.Collins (Cincinnati Children's Hospital) for histological assessments and advice. We also thank S. Hottinger (Cincinnati Children's Hospital) for editorial assistance, all of the participating families, the Cincinnati Center for Eosinophilic Disorders, and members of the Division of Allergy and Immunology.

Funding: This work was supported in part by NIH R37 AI045898, U19 AI070235, R01 AI057803, R01 DK107502, and P30 DK078392 (Gene and Protein Expression Core); the Campaign Urging Research for Eosinophilic Disease; the Buckeye Foundation; and the Sunshine Charitable Foundation and its supporters, Denise and David Bunning.

REFERENCES

1. Hammad H, Lambrecht BN, Barrier epithelial cells and the control of type 2 immunity. Immunity 43, 29–40 (2015).26200011
2. Samuelov L, Sarig O, Harmon RM, Rapaport D, Ishida-Yamamoto A, Isakov O, Koetsier JL, Gat A, Goldberg I, Bergman R, Spiegel R, Eytan O, Geller S, Peleg S, Shomron N, Goh CSM, Wilson NJ, Smith FJD, Pohler E, Simpson MA,McLean WHI, Irvine AD, Horowitz M, McGrath JA, Green KJ, Sprecher E, Desmoglein 1 deficiency results in severe dermatitis, multiple allergies and metabolic wasting. Nat. Genet 45, 1244–1248 (2013).23974871
3. Liacouras CA, Furuta GT, Hirano I, Atkins D, Attwood SE, Bonis PA, Burks AW,Chehade M, Collins MH, Dellon ES, Dohil R, Falk GW, Gonsalves N, Gupta SK, Katzka DA, Lucendo AJ, Markowitz JE, Noel RJ, Odze RD, Putnam PE, Richter JE, Romero Y, Ruchelli E, Sampson HA, Schoepfer A, Shaheen NJ, Sicherer SH, Spechler S, Spergel JM, Straumann A, Wershil BK, Rothenberg ME, Aceves SS, Eosinophilic esophagitis: Updated consensus recommendations for children and adults. J. Allergy Clin. Immunol 128, 3–20.e6 (2011).21477849

4. Martin LJ, Franciosi JP, Collins MH, Abonia JP, Lee JJ, Hommel KA, Varni JW, Grotjan JT, Eby M, He H, Marsolo K, Putnam PE, Garza JM, Kaul A, Wen T, Rothenberg ME, Pediatric Eosinophilic Esophagitis Symptom Scores (PEESS v2.0) identify histologic and molecular correlates of the key clinical features of disease. J. Allergy Clin. Immunol 135, 1519–1528.e8 (2015).26051952
5. Aceves SS, Chen D, Newbury RO, Dohil R, Bastian JF, Broide DH, Mast cells infiltrate the esophageal smooth muscle in patients with eosinophilic esophagitis, express TGF-β1, and increase esophageal smooth muscle contraction. J. Allergy Clin. Immunol 126, 1198–1204.e4 (2010). 21047675
6. Wen T, Kuhl J, Putnam P, Mukkada V, Farrell M, Kaul A, Cole C, Rothenberg ME, A flow cytometry-based diagnosis of eosinophilic esophagitis. J. Allergy Clin. Immunol 140, 1736–1739.e3 (2017).28826772
7. Katzka DA, Ravi K, Geno DM, Smyrk TC, Iyer PG, Alexander JA, Mabary JE, Camilleri M, Vaezi MF, Endoscopic mucosal impedance measurements correlate with eosinophilia and dilation of intercellular spaces in patients with eosinophilic esophagitis. Clin. Gastroenterol. Hepatol 13, 1242–1248.e1 (2015).25592662
8. Capocelli KE, Fernando SD, Menard-Katcher C, Furuta GT, Masterson JC, Wartchow EP, Ultrastructural features of eosinophilic oesophagitis: Impact of treatment on desmosomes. J. Clin. Pathol 68, 51–56 (2015)25359789
9. Sherrill JD, Kc K, Wu D, Djukic Z, Caldwell JM, Stucke EM, Kemme KA, Costello MS, Mingler MK, Blanchard C, Collins MH, Abonia JP, Putnam PE, Dellon ES, Orlando RC, Hogan SP, Rothenberg ME, Desmoglein-1 regulates esophageal epithelial barrier function and immune responses in eosinophilic esophagitis. Mucosal Immunol. 7, 718–729 (2014).24220297
10. Rothenberg ME, Spergel JM, Sherrill JD, Annaiah K, Martin LJ, Cianferoni A, Gober L, Kim C, Glessner J, Frackelton E, Thomas K, Blanchard C, Liacouras C,Verma R, Aceves S, Collins MH, Brown-Whitehorn T, Putnam PE, Franciosi JP,Chiavacci RM, Grant SF, Abonia JP, Sleiman PM, Hakonarson H, Common variants at 5q22 associate with pediatric eosinophilic esophagitis. Nat. Genet 42, 289–291 (2010).20208534
11. Davis BP, Stucke EM, Khorki ME, Litosh VA, Rymer JK, Rochman M, Travers J, Kottyan LC, Rothenberg ME, Eosinophilic esophagitis-linked calpain 14 is an IL-13-induced protease that mediates esophageal epithelial barrier impairment.JCI Insight 1, e86355 (2016).27158675
12. Cheng X, Lu SH, Cui Y, ECRG2 regulates ECM degradation and uPAR/FPRL1 pathway contributing cell invasion/migration. Cancer Lett. 290, 87–95 (2010).19796867
13. Huang G, Hu Z, Li M, Cui Y, Li Y, Guo L, Jiang W, Lu SH, ECRG2 inhibits cancer cell migration, invasion and metastasis through the down-regulation of uPA/plasmin activity. Carcinogenesis 28, 2274–2281 (2007).17602171
14. Chavanas S, Bodemer C, Rochat A, Hamel-Teillac D, Ali M, Irvine AD, Bonafe JL, Wilkinson J, Taieb A, Barrandon Y, Harper JI, de Prost Y, Hovnanian A, Mutations in *SPINK5,* encoding a serine protease inhibitor, cause Netherton syndrome. Nat. Genet 25, 141–142 (2000).10835624
15. Hannula-Jouppi K, Laasanen SL, Heikkila H, Tuomiranta M, Tuomi ML, Hilvo S, Kluger N, Kivirikko S, Hovnanian A, Makinen-Kiljunen S, Ranki A, IgE allergen component-based profiling and atopic manifestations in patients with Netherton syndrome. J. Allergy Clin. Immunol 134, 985–988 (2014).25159469
16. Paluel-Marmont C, Bellon N, Barbet P, Leclerc-Mercier S, Hadj-Rabia S, Dupont C, Bodemer C, Eosinophilic esophagitis and colonic mucosal eosinophilia in Netherton syndrome. J. Allergy Clin. Immunol 139, 2003–2005.e1 (2016).28025013
17. Wen T, Stucke EM, Grotjan TM, Kemme KA, Abonia JP, Putnam PE, Franciosi JP, Garza JM, Kaul A, King EC, Collins MH, Kushner JP, Rothenberg ME, Molecular diagnosis of eosinophilic esophagitis by gene expression profiling. Gastroenterology 145, 1289–1299 (2013).23978633
18. Blanchard C, Mingler MK, Vicario M, Abonia JP, Wu YY, Lu TX, Collins MH, Putnam PE, Wells SI, Rothenberg ME, IL-13 involvement in eosinophilic esophagitis: Transcriptome analysis and reversibility with glucocorticoids. J. Allergy Clin. Immunol 120, 1292–1300 (2007).18073124
19. Sun BK, Boxer LD, Ransohoff JD, Siprashvili Z, Qu K, Lopez-Pajares V, Hollmig ST, Khavari PA, CALML5 is a ZNF750- and TINCR-induced protein that binds stratifin to regulate epidermal differentiation. Genes Dev. 29, 2225–2230 (2015).26545810

20. Blanchard C, Stucke EM, Burwinkel K, Caldwell JM, Collins MH, Ahrens A, Buckmeier BK, Jameson SC, Greenberg A, Kaul A, Franciosi JP, Kushner JP, Martin LJ, Putnam PE, Abonia JP, Wells SI, Rothenberg ME, Coordinate interaction between IL-13 and epithelial differentiation cluster genes in eosinophilic esophagitis. J. Immunol 184, 4033–4041 (2010).20208004
21. Kc K, Rothenberg ME, Sherrill JD, In vitro model for studying esophageal epithelial differentiation and allergic inflammatory responses identifies keratin involvement in eosinophilic esophagitis. PLOS ONE 10, e0127755 (2015).26039063
22. Rothenberg ME, Wen T, Greenberg A, Alpan O, Enav B, Hirano I, Nadeau K, Kaiser S, Peters T, Perez A, Jones I, Arm JP, Strieter RM, Sabo R, Gunawardena KA, Intravenous anti-IL-13 mAb QAX576 for the treatment of eosinophilic esophagitis. J.Allergy Clin. Immunol 135, 500–507 (2015).25226850
23. Sehmi R, Cromwell O, Wardlaw AJ, Moqbel R, Kay AB, Interleukin-8 is a chemo-attractant for eosinophils purified from subjects with a blood eosinophilia but not from normal healthy subjects. Clin. Exp. Allergy 23, 1027–1036 (1993).10779297
24. Persad R, Huynh HQ, Hao L, Ha JR, Sergi C, Srivastava R, Persad S, Angiogenic remodeling in pediatric EoE is associated with increased levels of VEGF-A, angiogenin, IL-8, and activation of the TNF-α-NFκB pathway. J. Pediatr. Gastroenterol. Nutr 55, 251–260 (2012).22331014
25. Kagalwalla AF, Akhtar N, Woodruff SA, Rea BA, Masterson JC, Mukkada V, Parashette KR, Du J, Fillon S, Protheroe CA, Lee JJ, Amsden K, Melin-Aldana H, Capocelli KE, Furuta GT, Ackerman SJ, Eosinophilic esophagitis: Epithelial mesenchymal transition contributes to esophageal remodeling and reverses with treatment. J. Allergy Clin. Immunol 129, 1387–1396.e7 (2012). 22465212
26. Kottyan LC, Davis BP, Sherrill JD, Liu K, Rochman M, Kaufman K, Weirauch MT, Vaughn S, Lazaro S, Rupert AM, Kohram M, Stucke EM, Kemme KA, Magnusen A, He H, Dexheimer P, Chehade M, Wood RA, Pesek RD, Vickery BP, Fleischer DM, Lindbad R, Sampson HA, Mukkada VA, Putnam PE, Abonia JP, Martin LJ, Harley JB, Rothenberg ME, Genome-wide association analysis of eosinophilic esophagitis provides insight into the tissue specificity of this allergic disease. Nat. Genet 46, 895–900 (2014).25017104
27. Lewis EC, Expanding the clinical indications for α_1-arantitrypsin therapy. Mol. Med 18, 957–970 (2012).22634722
28. Hemani G, Shakhbazov K, Westra H-J, Esko T, Henders AK, McRae AF, Yang J, Gibson G, Martin NG, Metspalu A, Franke L, Montgomery GW, Visscher PM, Powell JE, Detection and replication of epistasis influencing transcription in humans. Nature 508, 249–253 (2014).24572353
29. Sherrill JD, Gao PS, Stucke EM, Blanchard C, Collins MH, Putnam PE, Franciosi JP, Kushner JP, Abonia JP, Assa'ad AH, Kovacic MB, Biagini Myers JM, Bochner BS, He H, Hershey GK, Martin LJ, Rothenberg ME, Variants of thymic stromal lymphopoietin and its receptor associate with eosinophilic esophagitis. J. Allergy Clin. Immunol 126, 160–165 e163 (2010).20620568
30. Furio L, de Veer S, Jaillet M, Briot A, Robin A, Deraison C, Hovnanian A, Transgenic kallikrein 5 mice reproduce major cutaneous and systemic hallmarks of Netherton syndrome. J. Exp. Med 211,499–513 (2014).24534191
31. Uhlen M, Fagerberg L, Hallström BM, Lindskog C, Oksvold P, Mardinoglu A, Sivertsson A, Kampf C, Sjöstedt E, Asplund A, Olsson I, Edlund K, Lundberg E, Navani S, Szigyarto CA, Odeberg J, Djureinovic D, Takanen JO, Hober S, Alm T, Edqvist P-H, Berling H, Tegel H, Mulder J, Rockberg J, Nilsson P, Schwenk JM, Hamsten M, von Feilitzen K, Forsberg M, Persson L, Johansson F, Zwahlen M, von Heijne G, Nielsen J, Pontén F, Proteomics. Tissue-based map of the human proteome. Science 347, 1260419 (2015).25613900
32. McAleer MA, Irvine AD, The multifunctional role of filaggrin in allergic skin disease. J. Allergy Clin. Immunol 131,280–291 (2013).23374260
33. Cheng X, Shen Z, Yang J, Lu S-H, Cui Y, ECRG2 disruption leads to centrosome amplification and spindle checkpoint defects contributing chromosome instability. J. Biol. Chem 283, 5888–5898 (2008).18162463
34. Alexander RA, Prager GW, Mihaly-Bison J, Uhrin P, Sunzenauer S, Binder BR, Schütz GJ, Freissmuth M, Breuss JM, VEGF-induced endothelial cell migration requires urokinase receptor (uPAR)-dependent integrin redistribution. Cardiovasc. Res 94, 125–135 (2012).22287577

35. Chabot V, Dromard C, Rico A, Langonné A, Gaillard J, Guilloton F, Casteilla L, Sensebé L, Urokinase-type plasminogen activator receptor interaction with β1 integrin is required for platelet-derived growth factor-AB-induced human mesenchymal stem/stromal cell migration. Stem Cell Res. Ther 6, 188 (2015).26420039

36. Stewart CE, Nijmeh HS, Brightling CE, Sayers I, uPAR regulates bronchial epithelial repair in vitro and is elevated in asthmatic epithelium. Thorax 67, 477–487 (2012).22139533

37. Blanchard C, Stucke EM, Rodriguez-Jimenez B, Burwinkel K, Collins MH, Ahrens A, Alexander ES, Butz BK, Jameson SC, Kaul A, Franciosi JP, Kushner JP, Putnam PE, Abonia JP, Rothenberg ME, A striking local esophageal cytokine expression profile in eosinophilic esophagitis. J. Allergy Clin. Immunol 127, 208–217.e1–7 (2011).21211656

38. Lucchesi C, Sheikh MS, Huang Y, Negative regulation of RNA-binding protein HuR by tumor-suppressor ECRG2. Oncogene 35, 2565–2573 (2016).26434587

39. Atasoy U, Curry SL, Lôpez de Silanes I, Shyu A-B, Casolaro V, Gorospe M, Stellato C, Regulation of eotaxin gene expression by TNF-α and IL-4 through mRNA stabilization: Involvement of the RNA-binding protein HuR. J. Immunol 171,4369–4378 (2003).14530362

40. Kovacic MB, Myers JM, Wang N, Martin LJ, Lindsey M, Ericksen MB, He H, Patterson TL, Baye TM, Torgerson D, Roth LA, Gupta J, Sivaprasad U, Gibson AM, Tsoras AM, Hu D, Eng C, Chapela R, Rodriguez-Santana JR, Rodriguez-Cintrôn W, Avila PC, Beckman K, Seibold MA, Gignoux C, Musaad SM, Chen W, Burchard EG, Hershey GK, Identification of KIF3A as a novel candidate gene for childhood asthma using RNA expression and population allelic frequencies differences. PLOS ONE 6, e23714 (2011).21912604

41. Ran FA, Hsu PD, Wright J, Agarwala V, Scott DA, Zhang F, Genome engineering using the CRISPR-Cas9 system. Nat. Protoc 8, 2281–2308 (2013).24157548

42. Kartashov AV, Barski A, BioWardrobe: An integrated platform for analysis of epigenomics and transcriptomics data. Genome Biol. 16, 158 (2015).26248465

43. Chen J, Bardes EE, Aronow BJ, Jegga AG, ToppGene Suite for gene list enrichment analysis and candidate gene prioritization. Nucleic Acids Res. 37, W305–W311 (2009).19465376

44. Wu D, Ahrens R, Osterfeld H, Noah TK, Groschwitz K, Foster PS, Steinbrecher KA, Rothenberg ME, Shroyer NF, Matthaei KI, Finkelman FD, Hogan SP, Interleukin-13 (IL-13)/IL-13 receptor α1 (IL-13Rα1) signaling regulates intestinal epithelial cystic fibrosis transmembrane conductance regulator channel-dependent Cl secretion. J. Biol. Chem 286, 13357–13369 (2011).21303908

45. Price AL, Patterson NJ, Plenge RM, Weinblatt ME, Shadick NA, Reich D, Principal components analysis corrects for stratification in genome-wide association studies. Nat. Genet 38, 904–909 (2006).16862161

46. Blanchard C, Wang N, Stringer KF, Mishra A, Fulkerson PC, Abonia JP, Jameson SC, Kirby C, Konikoff MR, Collins MH, Cohen MB, Akers R, Hogan SP, Assa'ad AH, Putnam PE, Aronow BJ, Rothenberg ME, Eotaxin-3 and a uniquely conserved gene-expression profile in eosinophilic esophagitis. J. Clin. Invest 116, 536–547 (2006).16453027

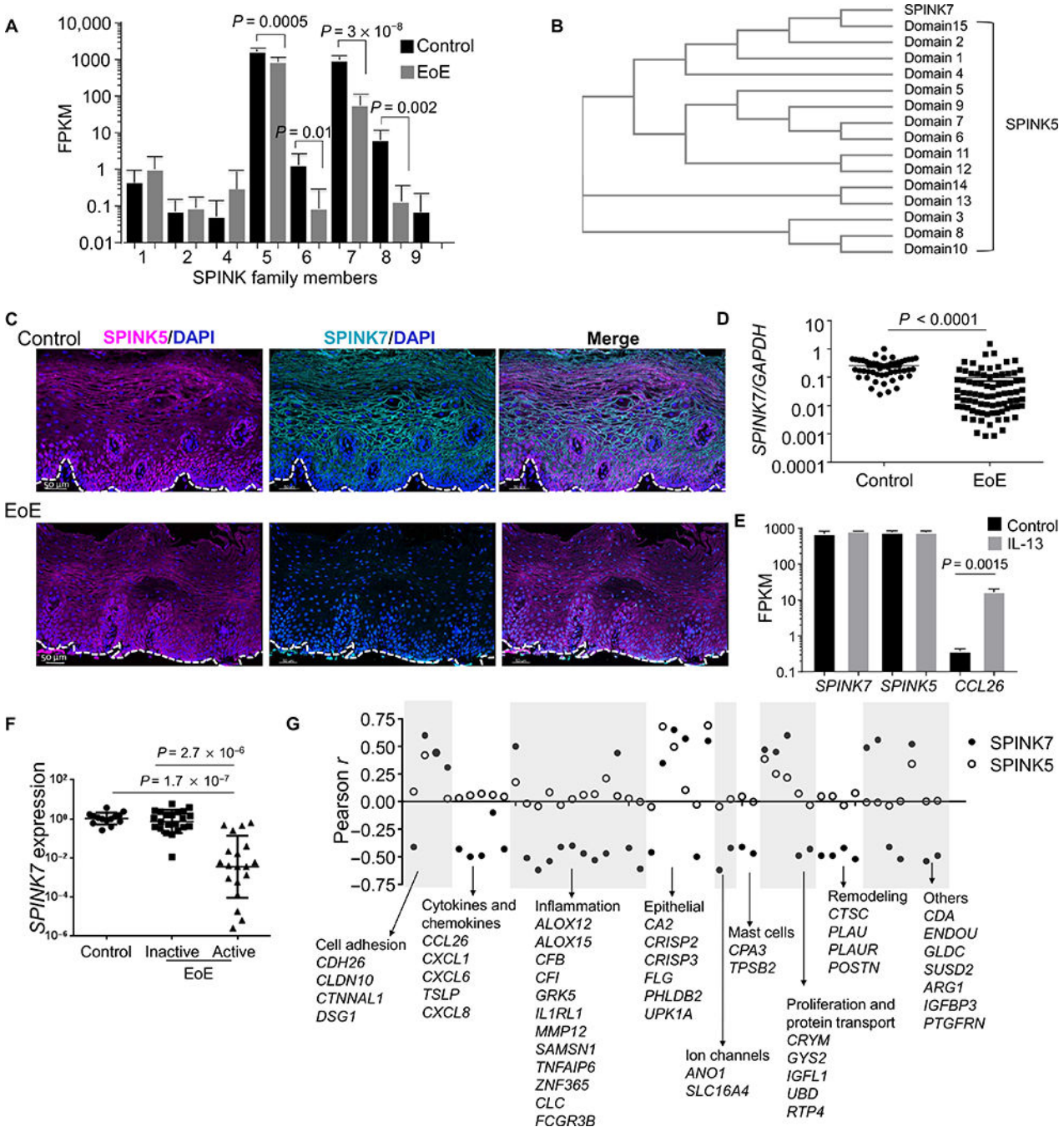

Fig. 1. Expression *of SPINK5* and *SPINK7* genes in EoE and their sequence analysis.

(**A**) FPKM values for *SPINK* family members determined from RNA-seq of esophageal biopsies *[n* = 6 control patients having 0 eosinophils per high-power field (control) and *n* = 10 patients with active EoE]. Data are means ± SD. *P* value was calculated by *t* test (unpaired, two-tailed). (**B**) Phylogenetic distribution of kazal domains ofSPINK5 and SPINK7. A molecular dendrogram of kazal domains was drawn by using the ClustalΩ program set at the default parameters. (**C**) Immunofluorescence staining of esophageal biopsy sections for SPINK5 (magenta) and SPINK7 (cyan) with 4′,6-diamidino-2-

phenylindole (DAPI)-stained nuclei (blue); representative images of four sections from different control patients and four sections from different patients with EoE are shown. The white dashed line separates the epithelium from the lamina propria. (**D**) Normalized *SPINK7* mRNA expression values (n = 50 control patients and *n* = 83 patients with EoE). Each point represents an individual patient. Statistical significance was calculated according to the Mann-Whitney *U* test. (**E**) FPKM values of *SPINK5, SPINK7,* and *CCL26* in differentiated EPC2 cells that were either untreated or treated with IL-13 (100 ng/ml) every other day for 7 days. *P* value was calculated by *t* test (unpaired, two-tailed) (**F**) SPINK7 mRNA expression from esophageal biopsies from 14 healthy controls, 22 patients with inactive EoE, and 19 patients with active EoE. *P* value was calculated by *t* test (unpaired, two-tailed). (**G**) Correlation of *SPINK5* and *SPINK7* expression with other EoE transcriptome genes as assessed by the EoE diagnostic panel (17) (*n* = 85 control and EoE patients) using Spearman correlations.

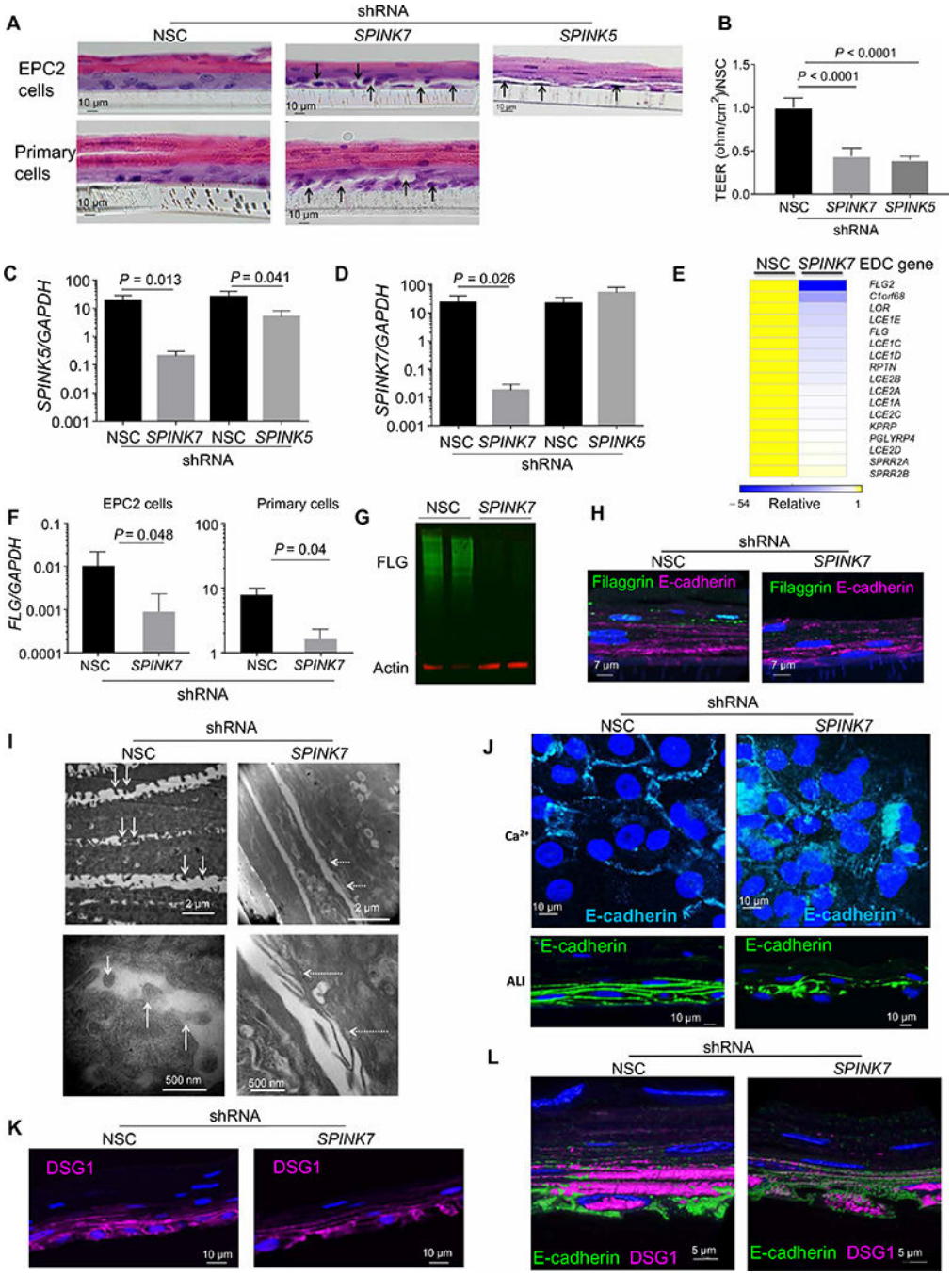

Fig. 2. Loss of *SPINK5* and *SPINK7* affects epithelial barrier function and architecture.

(**A**) Hematoxylin and eosin (H&E)-stained sections of either NSC-treated, *SPINK5*-silenced, or SPINK7-silenced EPC2 cells and primary esophageal epithelial cells after ALI differentiation (day 14). Arrows point to the noncellular areas that were formed. (**B**) TEER(ohm/cm^2) measurement from NSC-treated, SPINK7-silenced, and *SPINK5*- silenced EPC2 cells at day 7 of ALI differentiation. Data are the means ± SD from three independent experiments performed in triplicate. *P* value was calculated by *t* test (unpaired, two-tailed). Quantitative polymerase chain reaction (PCR) analysis of *SPINK5* expression (**C**) or

SPINK7 expression (**D**) of control (NSC), *SPINK7*- silenced, and *SPINK5*-silenced EPC2 cells that were grown for 14 days in ALI culture. Data are the means ± SD of three independent experiments performed in triplicate. *P* value was calculated by *t* test (unpaired, two-tailed). (**E**) A heatmap representing the fold change of 17 EDC genes that are significantly ($P < 0.05$) altered by *SPINK7* depletion in EPC2 cells after ALI differentiation (day 14) from three independent experiments. (**F**) *FLG* mRNA expression in NSC- treated or *SPINK7*-silenced EPC2 or primary esophageal epithelial cells obtained from control patients after ALI differentiation. Data are means ± SD. *P* value was calculated by *t* test (unpaired, two-tailed). (**G**) FLG protein expression in NSC-treated or *SPINK7*-silenced EPC2 cells after ALI differentiation was assessed by Western blot. (**H**) Representative images of coimmunofluorescence of FLG (green), E-cadherin (magenta), and nuclear DAPI stain (blue) in NSC- treated or *SPINK7*-silenced EPC2 cells after ALI differentiation. (**I**) Representative electron microscopy images of NSC-treated or SPINK7-silenced EPC2 cells after ALI differentiation (day 14) from three independent experiments. Arrows depict microplicae at the epithelial junctions. The dashed arrows depict the absence of microplicae at epithelial junctions. (**J**) Representative immunostained sections of E-cadherin (cyan and green) and DAPI (blue) of NSC-treated or *SPINK7*- silenced EPC2 cells grown with high Ca^{2+} (top) or after 14 days of ALI differentiations (bottom) from three independent experiments. (**K**) Representative immunostained sections of DAPI (blue) and DSG1 (magenta) of NSC-treated or SPINK7-silenced EPC2 cells after 14 days of ALI differentiation from three independent experiments. (**L**) Reconstituted three-dimensional confocal images of NSC-treated or SPINK7-silenced EPC2 cells after ALI differentiation (day 14) stained with DAPI (blue), E-cadherin (green), and DSG1 (magenta). Movie presentations of the data are available in the Supplementary Materials (movies S1 and S2). Images were processed by Imaris software.

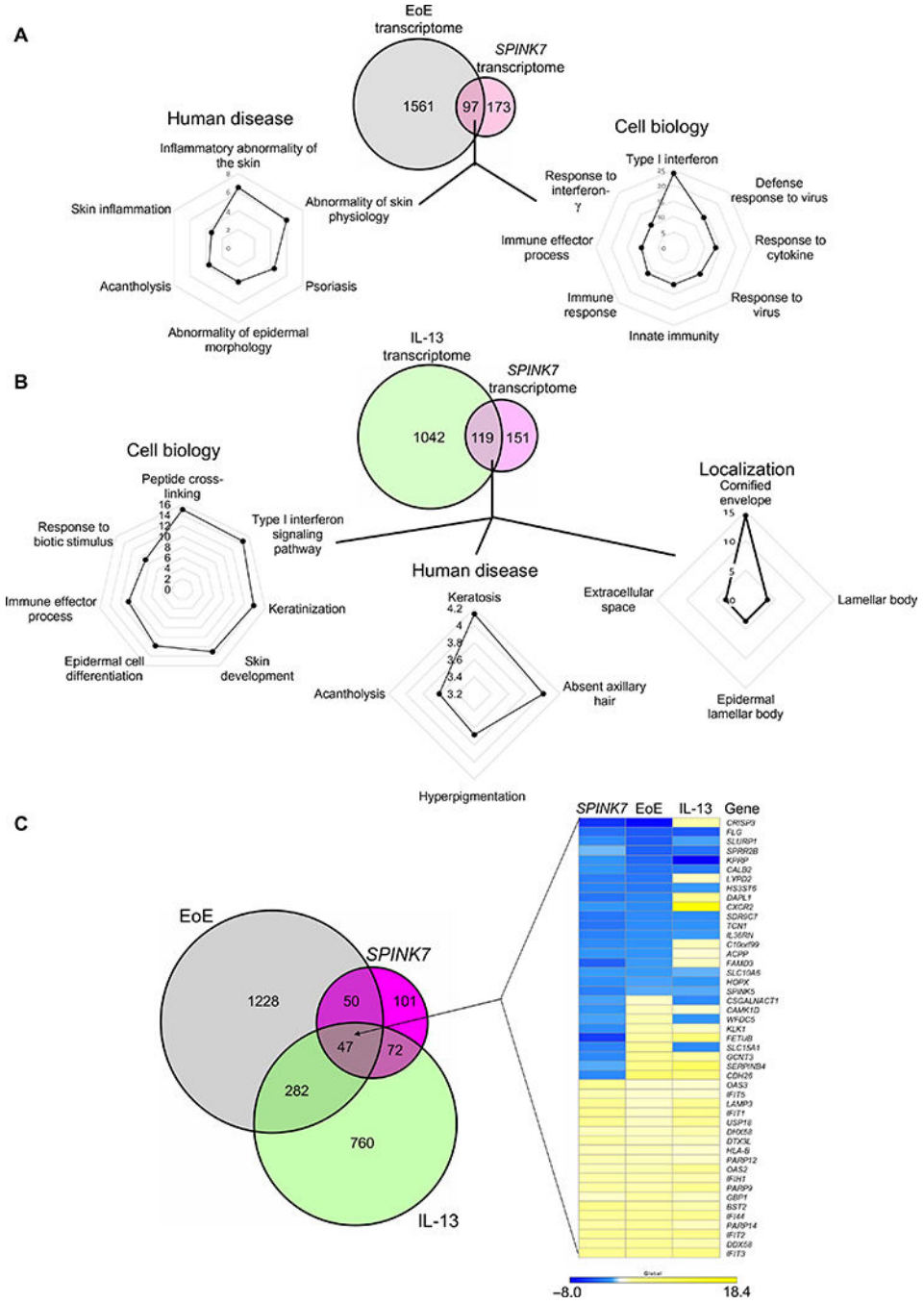

Fig. 3. Loss of *SPINK7* induces esophageal mucosa transcrip- tome centered on inflammation.

(**A**) Venn diagram depicting the number of genes differentially expressed (DE) as identified by RNA-seq of patients with EoE as compared to control (fold change > |2|, $P < 0.05$, FPKM > 1) [the EoE transcriptome has 1658 DE genes (9)] and in *SPINK7* gene silencing as compared to NSC treatment in EPC2 cells differentiated in ALI cultures for 14 days (*SPINK7* silencing has 270 DE genes). Genes overlapping between these two data sets were identified (97 genes). Gene ontology (GO) analyses of the *SPINK7-EoE* overlap gene set depicting human diseases or cell biology are presented according to the *P* values ($-\log_{10}$) for

pathway discovery. (**B**) Venn diagram depicting the number of genes DE as identified by RNA-seq of EPC2 cells after ALI differentiation after IL-13 stimulation compared to untreated cells (IL-13 was added starting from day 7 of the ALI cultures and was added three times per week in a concentration of 100 ng/ml) (fold change > |2|, $P < 0.05$, FPKM > 1) [the IL-13 transcriptome has 1161 DE genes (9)] and in *SPINK7* gene silencing as compared to NSC treatment in EPC2 cells differentiated in ALI cultures for 14 days *(SPINK7* silencing has DE 270 genes). Genes overlapping between these two data sets were identified (119 genes). GO analyses of the SPINK7-IL-13 overlap gene set depicting human diseases, cell biology, or localization is presented according to the *P* values ($-\log_{10}$) for pathway discovery. (**C**) Left: Venn diagram depicting the number of genes that overlap among EoE, *SPINK7* gene silencing, and IL-13 transcriptomes. Expression of the overlapping genes (47 genes) is represented by a heatmap (right) according to their fold change in *SPINK7* silencing as compared to NSC treatment, EoE as compared to control, or cells treated with IL-13 as compared to cells treated with vehicle (9)

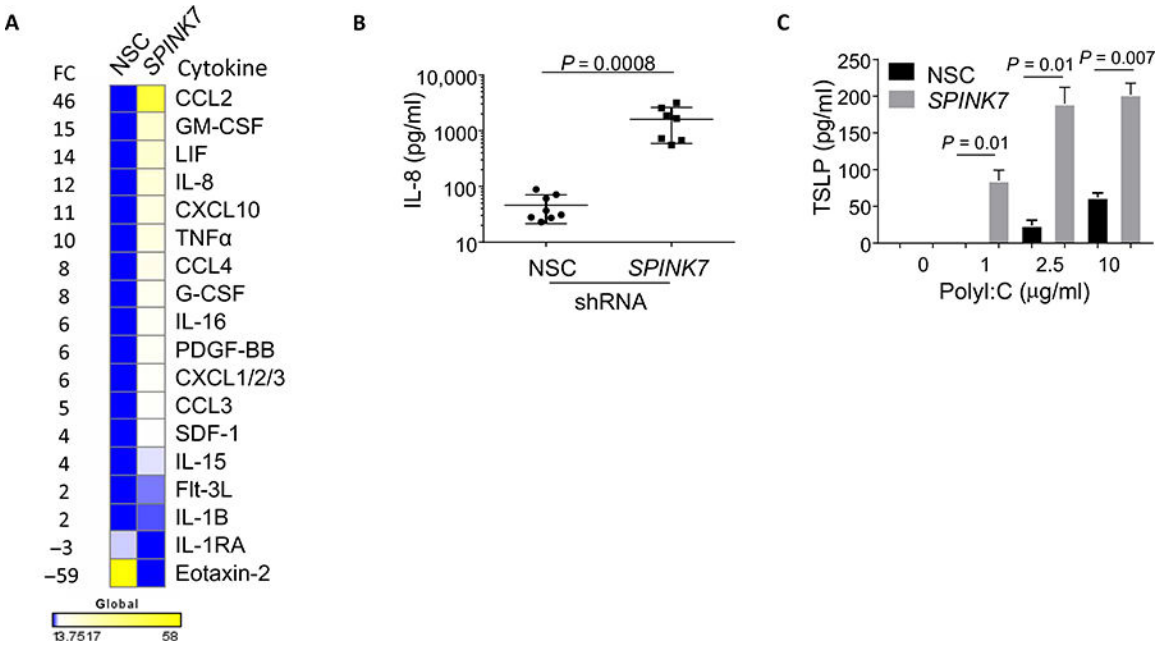

Fig. 4. Loss of *SPINK7* induces cytokine release.

(**A**) Heatmap of expression of cytokines and chemokines derived from supernatants of NSC-treated or SPINK7-silenced EPC2 cells after ALI differentiation (day 14) that were altered [all indicated cytokines and chemokines were expressed at a concentration >1 pg/ml, fold change (FC) > |2|, $P < 0.05$]. Data are presented as the mean fold change of *SPINK7* compared to NSC of three independent experiments performed in duplicate or triplicate. Blue, down-regulated cytokines after *SPINK7* silencing compared to NSC; yellow, up-regulated cytokines after *SPINK7* silencing compared to NSC. The label "CXCL1/2/3" represents the collective detection of CXCL1, CXCL2, and CXCL3. (**B**) IL-8 protein in supernatants from NSC-treated or *SPINK7*-silenced EPC2 cells after ALI differentiation (day 14). Each point represents one data point from three independent experiments performed in triplicate. (**C**) A representative experiment of TSLP release from EPC2 cells that were grown in high-calcium media for 64 hours and then stimulated for 8 hours with the indicated concentrations of polyinosinic-polycytidylic acid (polyI:C). Cell supernatants were assessed for TSLP levels from three independent experiments. Data are the means ± SD of a representative experiment. All *P* values were calculated by *t* test (unpaired, two-tailed).

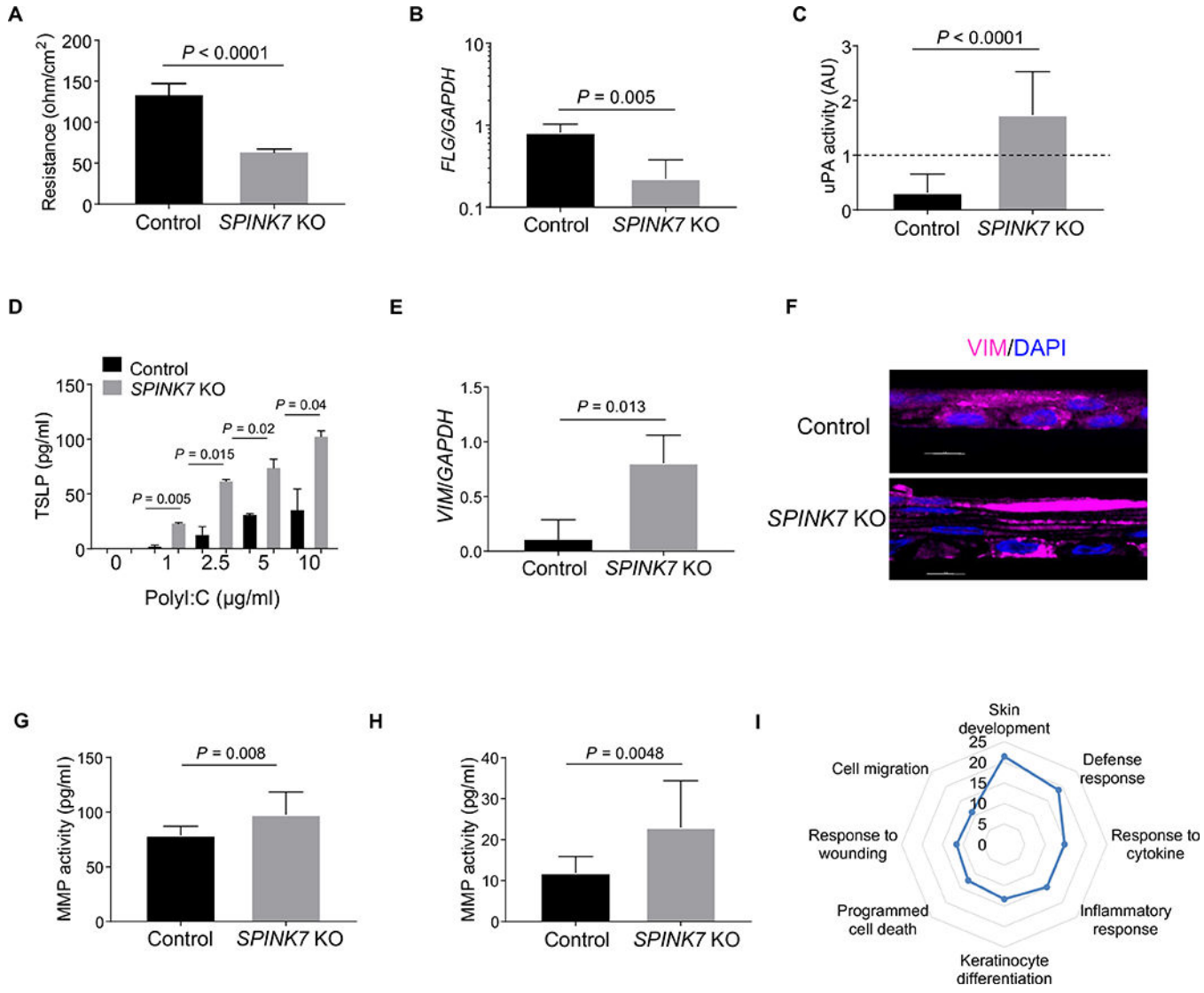

Fig. 5. *SPINK7* CRISPR/Cas9 KO cells phenocopy SPINK7-silenced cells and reveal induction of an EMT marker and increased MMP proteolytic activity.

(**A**) A representative TEER (ohm/cm^2) measurement from *SPINK7* CRISPR/Cas9 KO and control EPC2 cells at day 9 of ALI differentiation from three independent experiments performed in six replicates. Data are means ± SD. (**B**) *FLG* mRNA expression in control or *SPINK7-KO* EPC2 cells after ALI differentiation. Data are the means ± SD from four independent experiments performed in six replicates. (**C**) Quantification of uPA activity in supernatants derived from differentiated *SPINK7* KO and control EPC2 cells that were loaded with 1 active unit (AU) of purified uPA. uPA activity in the supernatants is calculated as AUs according to standard dilutions of uPA. The dashed line represents the amount of uPA that was added to the supernatants. Data are the means ± SD of a representative experiment from three independent experiments performed in six replicates. (**D**) Representative data of TSLP release from EPC2 cells that were grown in high-calcium media for 64 hours and then stimulated for 8 hours with the indicated concentrations of polyI:C. Cell supernatants were assessed for TSLP concentrations from three independent

experiments. Data are means ± SD. (**E**) *VIM* mRNA expression in control or *SPINK7-KO* EPC2 cells after ALI differentiation. Data are the means ± SD from four independent experiments. (**F**) Representative immunostained sections of DAPI (blue) and vimentin (VIM; magenta) of control NSC-treated or SPINK7-silenced EPC2 after 14 days of ALI differentiation from three independent experiments. Quantification of MMPs (**G**) or MMP9 (**H**) proteolytic activity in supernatants derived from NSC-treated or SPINK7-silenced EPC2 differentiated cells. MMP activity in the supernatants is calculated according to standard dilutions of MMP9. Data are the means ± SD of three independent experiments performed in triplicate. (**I**) GO analyses of the CRISPR/Cas9 *SPINK7* KO differentiated cells compared to CRISPR/Cas9 control cells. Numbers presented are the *P* values (−log10). All *P* values were calculated by *t* test (unpaired, two-tailed) except GO analysis, which uses analysis of variance (ANOVA) test.

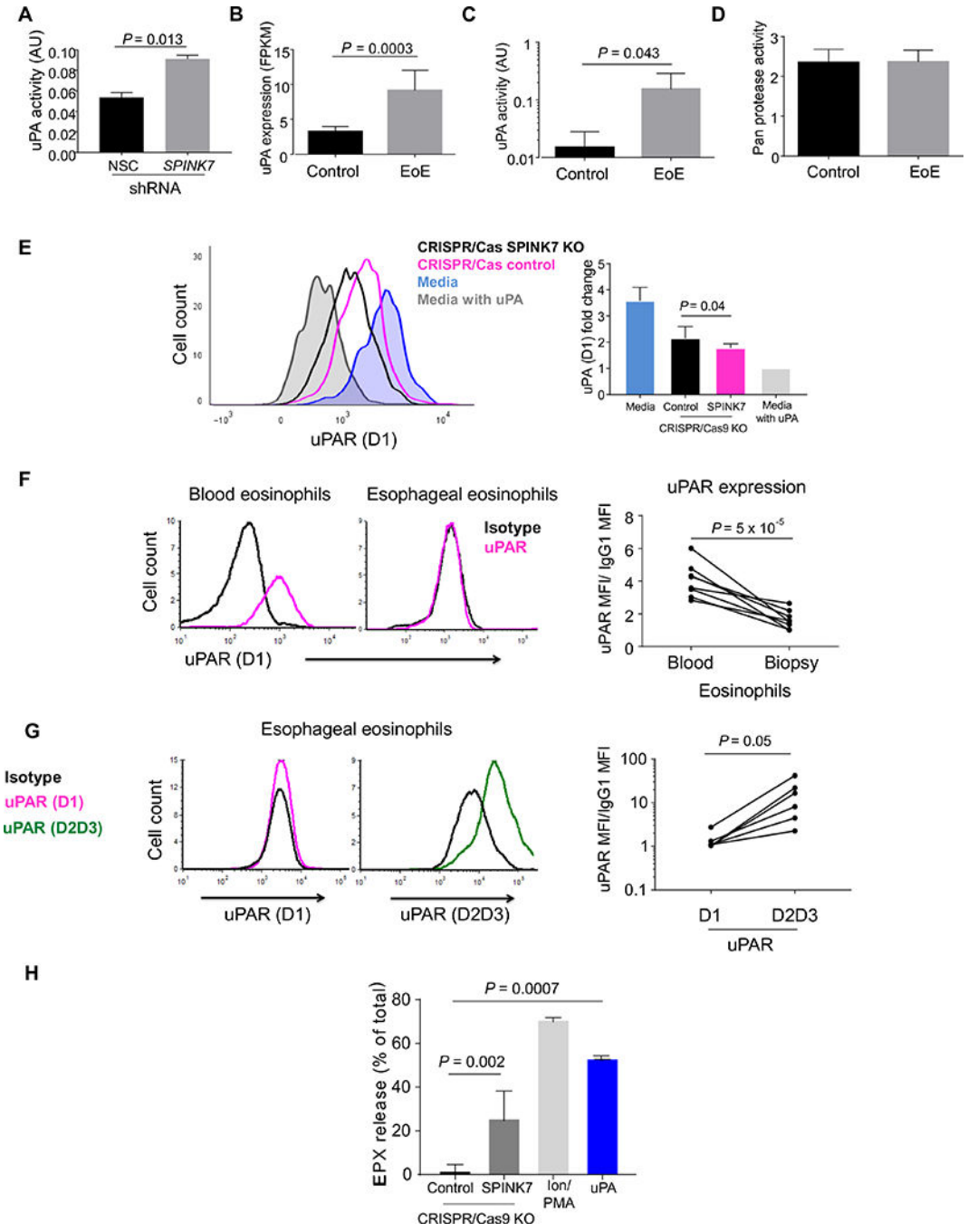

Fig. 6. SPINK7 regulates eosinophil function by regulating the uPA/uPAR pathway in the esophagus.

(**A**) Quantification of uPA activity in supernatants derived from NSC- treated or SPINK7-silenced EPC2 cells during ALI differentiation (days 7 to 9). uPA activity in the supernatants is calculated as AUs according to standard dilutions of uPA. Data are the means ± SD of three independent experiments performed in triplicate. *P* values were calculated by *t* test (unpaired, two-tailed). (**B**) FPKM values of uPA in the esophagus of patients with EoE (n = 8) and controls (n = 5). Data are means ± SD. *P* values were calculated by *t* test (unpaired,

two-tailed). (**C**) Analysis of the uPA proteolytic activity (AU) in esophageal biopsies from patients with EoE and control individuals (n = 6 for each cohort). Data are means ± SD. *P* values were calculated by *t* test (unpaired, two-tailed). (**D**) Analysis of the pan protease activity in esophageal biopsies from patients with EoE and control individuals (n = 6 for each cohort). (**E**) The expression of the D1 domain of uPAR was quantified [according to the mean fluorescence intensity (MFI) using flow cytometry] on the cell surface of eosinophils that were incubated with supernatants from control or *SPINK7* KO differentiated cells. (**F**) The expression of the D1 domain of uPAR was quantified (MFI using flow cytometry) on the cell surface of eosinophils ($7AAD^{low}$, CD45+, CD11B+, SIGLEC8+) derived from either blood or esophageal biopsies from patients with EoE (n = 8 individuals). Each point represents a single patient. *P* value was calculated by *t* test (paired, two-A and B). It is notable that uPA binds to its receptor uPAR on the D1 domain and cleaves uPAR. This cleavage results in exposure of a ligand on uPAR that promotes interaction with coreceptors such as the formyl peptide receptor-like 1 and cellular activation (12). We investigated the effects of uPA on the expression of uPAR. uPA decreased D1 domain expression on eosinophils in a dose-dependent manner and did nottailed). IgG1, immunoglobulin G1. (**G**) Using flow cytometry, expression of D1 and D2D3 domains of uPAR was quantified (according to the MFI) on the cell surface of eosinophils derived from esophageal biopsies of additional six patients with EoE. Each point represents a single patient. *P* value was calculated by *t* test (paired, two-tailed). (**H**) Supernatants derived from either *SPINK7* KO cells, control cells, or purified eosinophils treated with uPA (10 nM) or a combination of A23187 (10 mM) and phorbol 12-myristate 13-acetate (50 nM) (Ion + PMA), which induced the release of EPX from the eosinophils purified from blood of three healthy donors. Data are means ± SD. *P* value was calculated by *t* test (unpaired, two-tailed).

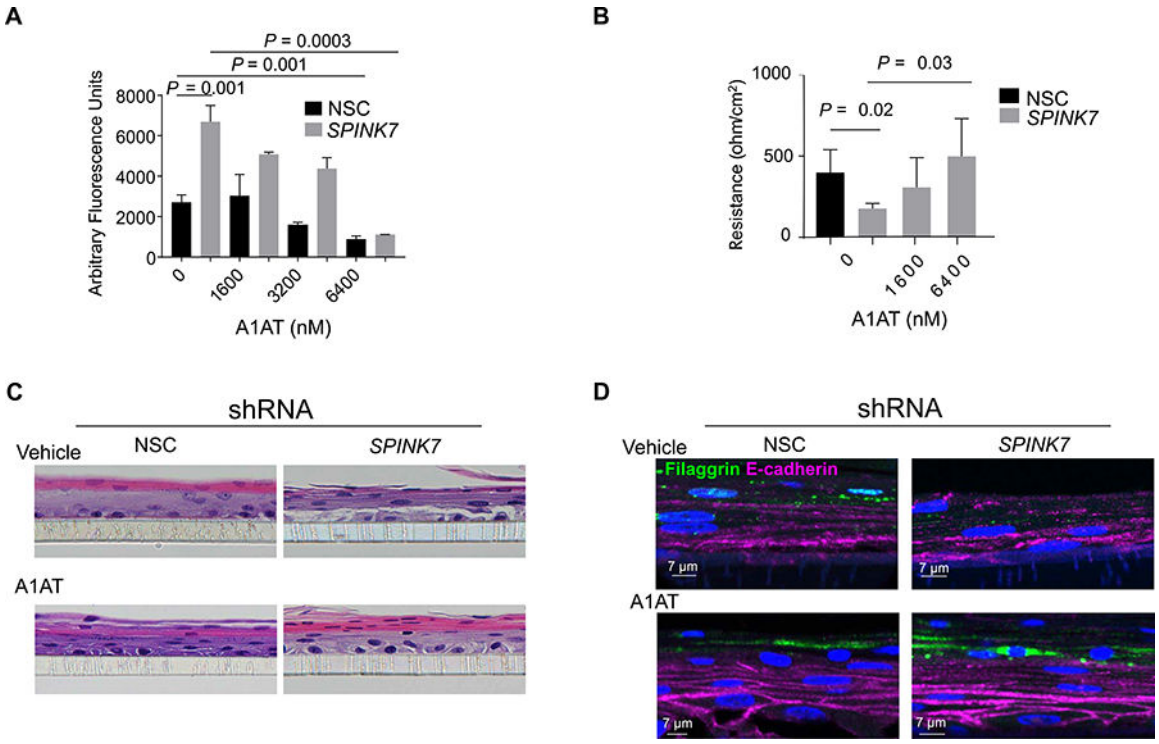

Fig. 7. A1AT administration ameliorates the effects caused by loss of *SPINK7*.

(**A**) Quantification of trypsin-like activity in supernatants derived from NSC-treated or *SPINK7*- silenced EPC2 cells that were treated with A1AT or vehicle after ALI differentiation. Data are the means ± SD of three independent experiments. (**B**) Electrical resistance measurements of NSC-treated or SPINK7-silenced EPC2 cells that were treated with A1AT or a vehicle during ALI differentiation. Data are means ± SD. (**C**) H&E staining of NSC-treated or SPINK7-silenced EPC2 cells that were treated with A1AT or a vehicle after ALI differentiation (day 14). (**D**) Coimmunofluorescence staining of E-cadherin (magenta) and FLG (green) of NSC-treated or SPINK7-silenced EPC2 cells that were treated with A1AT or vehicle after ALI differentiation. *P* values were calculated by *t* test (unpaired, two-tailed).

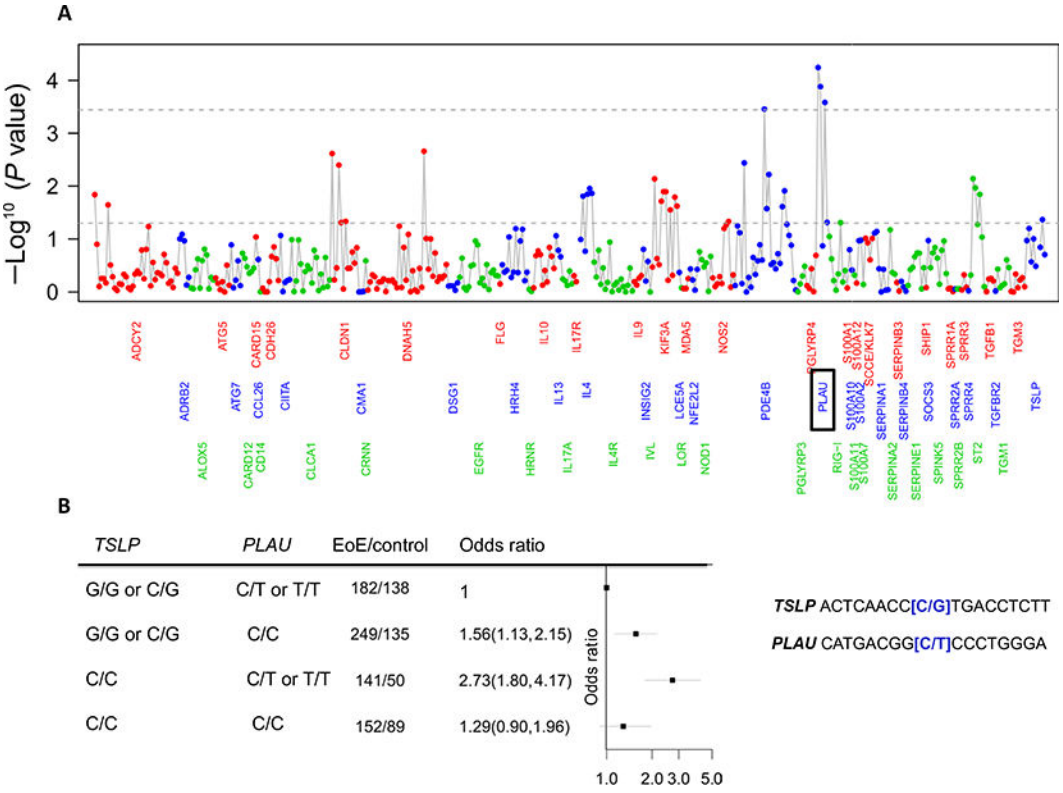

Fig. 8. Epistasis between genetic variants in *TSLP* and *PLAU* contributes to EoE susceptibility.

(**A**) Genetic interaction between *TSLP* (rs2289277) and SNPs in 68 atopy- related genes. Logistic regression analyses with interaction term were performed using 725 cases and 412 controls. Each circle represents a single SNP, which is colored according to its locus. Covariates include age, sex, and three principal components. Multiple testing threshold, $P < 0.00036$ is shown as the upper dashed line, whereas $P < 0.05$ is shown as the lower dashed line. The *PLAU* gene is denoted with a rectangle. (**B**) Forest plot evaluating the combinatorial effects of the presence of at least one minor allele at *TSLP* (rs2289277-G) and *PLAU* (rs2459449-T) and polymorphic sequences are shown.